Journal of Thermal Analysis, Vol. 38 (1992) 2437-2454

THERMAL DEHYDRATION AND DECOMPOSITION OF COBALT CHLORIDE HYDRATE ($CoCl_2 \cdot xH_2O$)

*S. K. Mishra and S. B. Kanungo**

REGIONAL RESEARCH LABORATORY, BHUBANESWAR-751 013, ORISSA, INDIA

(Received August 12, 1991)

Dehydration and decomposition of an undried and a partly dried sample of hydrated $CoCl_2$ have been investigated by using both isothermal and non-isothermal weight loss methods. The intermediate products of dehydration and decomposition at different temperatures have been characterized by chemical analysis, X-ray diffraction, microscopy, infrared and diffuse reflectance spectroscopy. Though XRD failed to identify clearly the formation of basic salt, infrared spectra reveal the occurrence of hydrogen bonded OH groups in the samples heated at even 500°–600°C. This is further supported from the diffuse reflectance spectra of "dehydrated" samples which indicate tetragonally distorted co-ordination structures due to the presence of H_2O. Thermodynamic functions for different steps of dehydration have been calculated and discussed in the light of structural changes taking place in the dehydrated salts.

Keywords: $CoCl_2 \cdot xH_2O$, mechanism of dehydration, thermodynamic parameters

Introduction

Thermal deaquation of $CoCl_2 \cdot 6H_2O$ has been the subject of considerable investigation by numerous authors mainly because it is one of the few hydrated salts which shows distinct steps of the loss of its water of crystallization in the temperature range of ambient to 200°C. Though it is generally agreed that hexahydrate shows three stages of dehydration in TG curve, there are some differences of opinion as to the mechanism of these thermal processes. Whereas some authors [1, 2] suggest that 2 mol of water are lost in each stage, others [3–6] believe that 4 mol of water are lost in the first stage and one mol of water in each

* Author to whom all correspondence should be addressed

John Wiley & Sons, Limited, Chichester
Akadémiai Kiadó, Budapest

of the two subsequent stages of weight loss. No literature information is available as to the mechanism of dehydration if a salt containing either more or less than six molecules of water is heated. Further, no information is available on the thermal decomposition behaviour of a partially dehydrated or an anhydrous $CoCl_2$. Since all these aspects are relevant in the selective chlorination and chloridization of cobalt bearing minerals, it was considered worthwhile to reexamine the thermal dehydration and decomposition behaviour of hydrated $CoCl_2$ not only in air but also in flowing nitrogen atmosphere. Attempts have also been made to characterize the intermediate products of decomposition and to derive thermodynamic parameters for each stage of the process.

Experimental

Materials

Both undried and partly dried analytical reagent grade $CoCl_2$ hydrate were used in the present work. The latter was prepared by drying the former in a dessicator for 7–8 days over concentrated sulphuric acid and phosphorus pentoxide. Chemical analyses reveal that the composition of the undried and dried samples are $CoCl_2 \cdot 7.33H_2O$ and $CoCl_2 \cdot 5.88H_2O$ respectively.

Methods

Various experimental procedures such as dehydration/decomposition by isothermal and non-isothermal methods, physico-chemical characterization of the intermediate products of decomposition were same as those used in the previous communication [7] on nickel chloride. Cobalt was estimated by titration with EDTA using xylenol orange as indicator and by AAS when present in small quantity. Chloride was estimated by titration with standard $AgNO_3$ solution and by ion-selective electrode (MICRO-2, England) when present in small quantity.

Results and discussion

Isothermal decomposition

Figure 1 illustrates isothermal weight loss behaviour of $CoCl_2 \cdot 7.33H_2O$ with respect to time. The nature of the rate curves is, in general, similar to those obtained for $NiCl_2 \cdot 7.55H_2O$ [7]. The initial rate of decomposition (upto 10 min) increases very sharply at all temperatures from 150° to 600°C. However, from 200° to 400°C the rate of weight loss decreases gradually after 10 min of heating and

reaches a nearly constant value from 20 to 60 min. It can be noted that the initial rate curves at 270° and 400°C are very close suggesting that at 250°–270°C hydrated $CoCl_2$ loses most of its water and the dehydrated salt is stable upto 400°C. At 500°C and above further loss in weight due to dechlorination takes place. At 600°C the maximum weight loss observed is about 68% against 69.2% at 800°C.

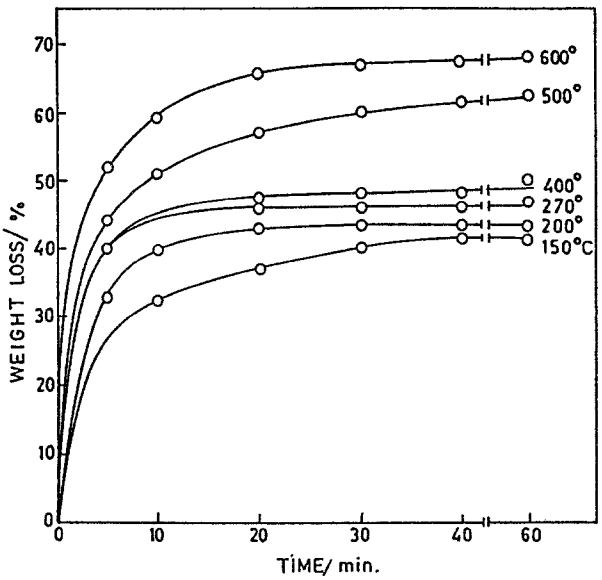

Fig. 1 Isothermal decomposition of $CoCl_2 \cdot 7.33\ H_2O$ in air

Non-isothermal decomposition

TG and DTA of the two samples in static air (Fig. 2) and flowing nitrogen (Fig. 3) demonstrate that the dehydration behaviour of hydrated $CoCl_2$ is almost similar in both the environments, although TG shows little more weight loss in flowing nitrogen. Five distinct endothermic effects can be noticed from ambient to 280°C for undried sample. The first one at 90°–95°C without any weight loss is due to incongruent melting of a portion of water of hydration in which the salt forms a saturated solution. The second peak at 125°–130°C is due to the loss of little less than one mole of water, a phenomenon which is absent in the thermogram of partly dried sample. This is followed by a large endothermic effect around 165°C corresponding to the loss of 4.33 mol of water for undried sample. The two subsequent endothermic effects at 200° and 240°C represent the loss of one mole of water each. For partly dried sample all the four endothermic peaks appear at temperatures 10°–15°C lower than those for the undried sample. In flowing nitrogen atmosphere the observed weight losses are little higher, possibly

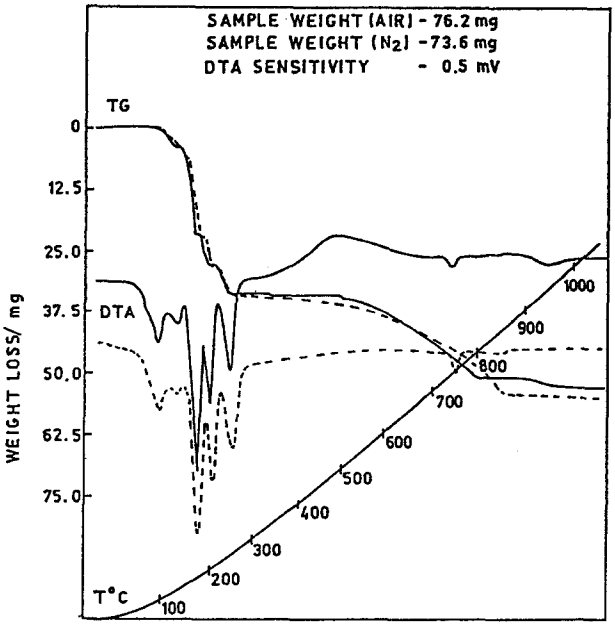

Fig. 2 Thermoanalytical curves of $CoCl_2 \cdot 7.33\ H_2O$. Solid line represents static air and broken line represents flowing nitrogen environments

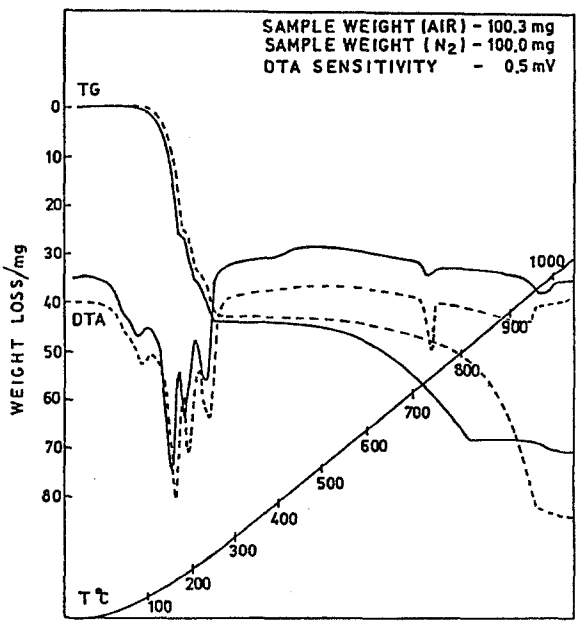

Fig. 3 Thermoanalytical curves of $CoCl_2 \cdot 5.88\ H_2O$. Solid line represents static air and broken line represents flowing nitrogen environments

due to more rapid evaporation. Figures 2 and 3 also show that from 280° to 400°C no loss in weight occurs suggesting the stability of anhydrous $CoCl_2$ in both the environments. This is also supported by the isothermal weight loss data.

The thermal effects above 300°C for $CoCl_2$ appear to be different from that of $NiCl_2$. A broad exothermic effect around 500°C in static air for undried sample corresponds with the beginning of weight loss due to decomposition (dehydrochlorination). Since in nitrogen atmosphere this effect is not perceptible it may be inferred that in static air decomposition of $CoCl_2$ and oxidation of CoO to Co_2O_3 takes place almost simultaneously. But this exothermic effect is not prominent for partly dried sample in air suggesting that a different mechanism of dechlorination for salts containing less than six molecules of water of hydration. The sharp endothermic effect at 730°–740°C particularly in N_2 atmosphere represents melting of anhydrous $CoCl_2$ [8, 9]. Heat of melting calculated from peak area for partly dried sample in N_2 atmosphere (Fig. 3) comes to about 10.0 $kJ \cdot mol^{-1}$ which is in excellent agreement with the literature value of 10.7 $kJ \cdot mol^{-1}$ [9]. In static air another small endothermic effect accompanied with 2.2% weight loss at 940°–960°C is possibly due to the decomposition of Co_2O_3 to

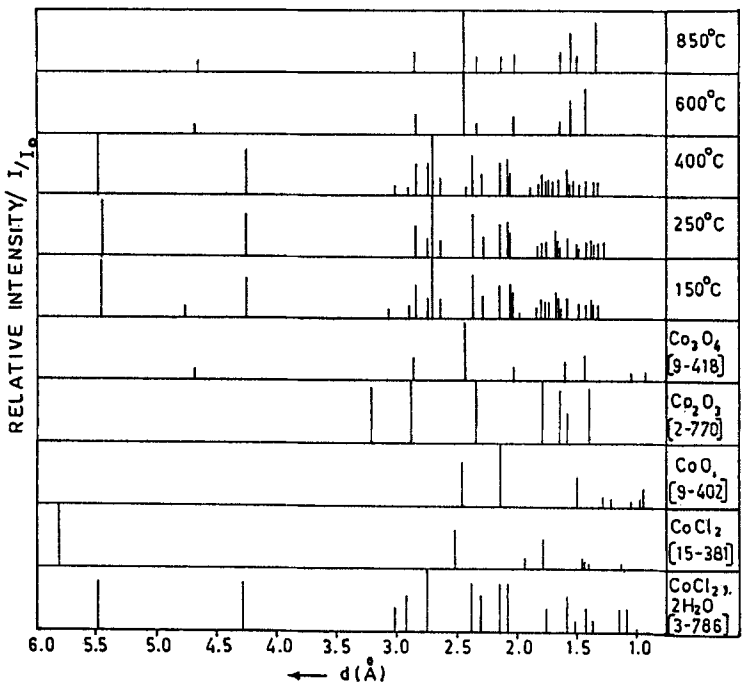

Fig. 4 X-ray diffraction pattern of $CoCl_2 \cdot 7.33\ H_2O$ calcined at different temperatures for 1 hour Standard diffractograms of possible intermediates are also included for reference

Table 1 Calculated and observed weight losses for different steps of dehydration and decomposition of $CoCl_2 \cdot 7.33\ H_2O$

Step No.	T / °C	Proposed steps of reactions	Cumulative weight loss / % in			
			Static air		Flowing nitrogen	
			Calculated	Observed	Calculated	Observed
1.	130	$CoCl_2 \cdot 7.33H_2O(s) \rightarrow CoCl_2 \cdot 6.63H_2O\ (l) + 0.70H_2O\ (v)$	4.81	4.91	–	–
	125	$CoCl_2 \cdot 7.33H_2O(s) \rightarrow CoCl_2 \cdot 6.58H_2O\ (l) + 0.75H_2O\ (v)$	–	–	5.15	5.10
2.	170	$CoCl_2 \cdot 6.63H_2O(l) \rightarrow CoCl_2 \cdot 3.23H_2O\ (s) + 3.40H_2O\ (v)$	28.18	28.21	–	–
	165	$CoCl_2 \cdot 6.58H_2O(l) \rightarrow CoCl_2 \cdot 3H_2O\ (s) + 3.58H_2O\ (v)$	–	–	29.75	29.89
3.	200	$CoCl_2 \cdot 3.23H_2O(s) \rightarrow CoCl_2 \cdot 2H_2O\ (s) + 1.23H_2O\ (v)$	36.62	36.42	–	–
	195	$CoCl_2 \cdot 3H_2O\ (s) \rightarrow CoCl_2 \cdot 1.8H_2O\ (s) + 1.20H_2O\ (v)$	–	–	38.00	38.21
4.	240	$CoCl_2 \cdot 2H_2O\ (s) \rightarrow CoCl_2 \cdot H_2O\ (s) + H_2O\ (v)$	43.49	44.29	–	–
	240	$CoCl_2 \cdot 1.8H_2O\ (s) \rightarrow CoCl_2 \cdot 0.5H_2O\ (s) + 1.30H_2O\ (v)$	–	–	46.94	46.36
5.	850	$2CoCl_2 \cdot H_2O\ (s) + \frac{1}{2}O_2\ (g) \rightarrow Co_2O_3\ (s) + 4HCl\ (g)$	69.22	69.21	–	–
	850	$2CoCl_2 \cdot 0.5H_2O\ (s) + \frac{1}{2}O_2\ (g) \rightarrow 2CoO + 2HCl(g) + Cl_2\ (g)$	–	–	72.23	73.00

Table 2 Calculated and observed weight losses for different steps of dehydration and decomposition of $CoCl_2 \cdot 5.88\ H_2O$

Step No.	T / °C	Proposed steps of reactions	Cumulative weight loss / % in Static air Calculated	Static air Observed	Flowing nitrogen Calculated	Flowing nitrogen Observed
1.	80	$CoCl_2 \cdot 5.88H_2O$ (s) $\rightarrow CoCl_2 \cdot 5.88H_2O$ (l)	–	–	–	–
2.	150	$CoCl_2 \cdot 5.88H_2O$ (l) $\rightarrow CoCl_2 \cdot 2.38H_2O$ (s)+ $3.50H_2O$ (v)	26.72	26.42	–	–
		$CoCl_2 \cdot 5.88H_2O$ (l) $\rightarrow CoCl_2 \cdot 2.53H_2O$ (s)+ $3.35H_2O$ (v)	–	–	25.57	25.52
3.	180	$CoCl_2 \cdot 2.38H_2O$ (s) $\rightarrow CoCl_2 \cdot 1.20H_2O$ (s)+ $1.18H_2O$ (v)	35.73	35.40	–	–
		$CoCl_2 \cdot 2.53H_2O$ (s) $\rightarrow CoCl_2 \cdot 1.23H_2O$ (s)+ $1.30H_2O$ (v)	–	–	35.50	35.10
4.	230	$CoCl_2 \cdot 1.20H_2O$ (s) $\rightarrow CoCl_2$ (s)+ $1.20H_2O$ (v)	44.86	44.36	–	–
		$CoCl_2 \cdot 1.23H_2O$ (s) $\rightarrow CoCl_2$ (s)+ $1.23H_2O$ (v)	–	–	44.50	44.86
5.	850	$2CoCl_2$ (l) + H_2O (v) + O_2 (g) $\rightarrow Co_2O_3$ (s) + Cl_2 (g)+ 2HCl (g)	–	–	–	–
	1050	$CoCl_2$ (l) + H_2O (v) $\rightarrow$ CoO (s) + 2HCl (v)	–	–	84.84	85.00

Co_3O_4. Tables 1 and 2 summarise the various reaction steps with their corresponding weight losses for undried and partly dried samples respectively.

Chemical analysis of the intermediate products

Chemical analysis of the products of isothermal decomposition at different temperatures support the general decomposition behaviour of $CoCl_2$ hydrate. The results in Table 3 show that there is no appreciable loss of chlorine upto 400°C confirming the observations made in the preceeding paragraphs. However, some loss of chlorine do takes place during dehydration even at temperature as low as 250° and at 500°C considerable loss of chlorine occurs. As the product of decomposition at temperatures higher than 500°C was not soluble in either dilute HNO_3 or in H_2SO_4 (possibly due to the formation of Co_2O_3) it was not possible to estimate chloride content and hence Cl/Co ratio could not be determined.

X-ray diffraction

X-ray diffraction patterns of the products of decomposition at different temperature are illustrated in Fig. 4. The figure suggests that $CoCl_2 \cdot 2H_2O$ is the major phase in the entire temperature range of 150°–400°C. This is because, anhydrous phase formed is converted to dihydrate by absorbing moisture from air during the preparation of sample for XRD analysis. At 600°C the major phase is Co_2O_3 with minor amounts of Co_3O_4, whereas at 850°C the major phase is Co_3O_4.

Table 3 Chemical analysis of the products of thermal decomposition of $CoCl_2 \cdot 7.33\ H_2O$ at different temperatures and their solubility in water

T/	Weight loss /	Co	Cl	Cl/Co	Solubility in water	
				mol	soluble in water	insoluble in water
°C	%	%	%	ratio	%	%
150	41.3	35.0	40.5	1.92	100	–
200	44.2	39.2	48.0	2.03	100	–
250	46.2	37.3	44.0	1.96	100	–
400	49.5	40.5	45.5	1.87	98.0	2.0
500	63.0	37.7	28.8	1.27	90.9	9.1
600	67.5				72.0	28.0

Infrared spectra

The infrared spectra of hydrated $CoCl_2$ calcined at different temperatures reveals better features than those of heat treated $NiCl_2$ [7]. It can be seen from Fig. 5 that at 200°C thoughts free water is the major component in the region of

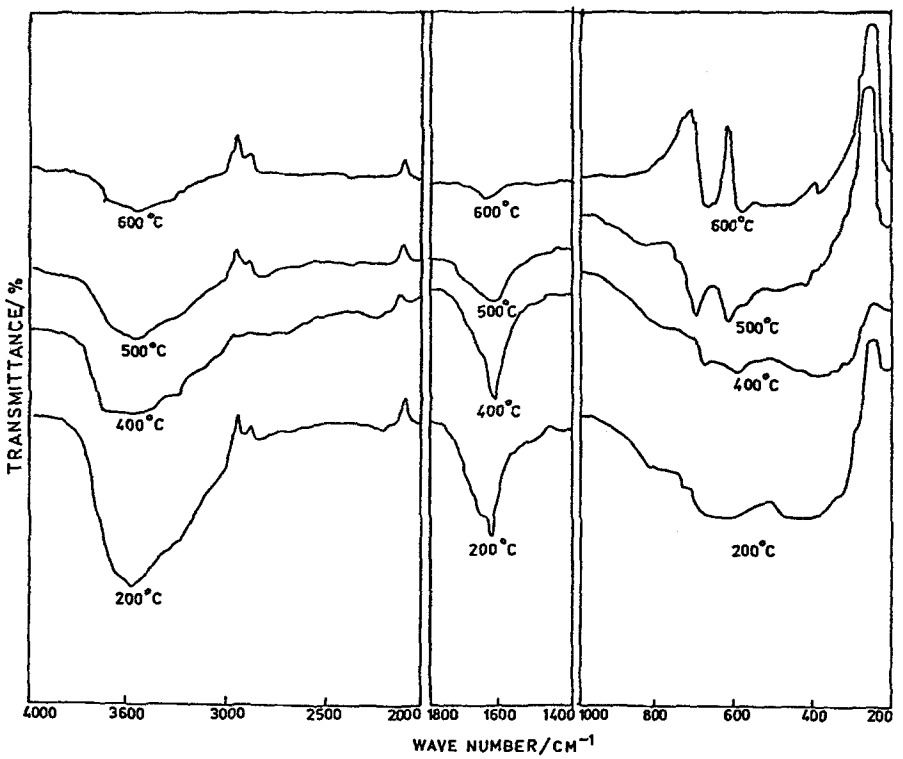

Fig. 5 IR-spectra of $CoCl_2 \cdot 7.33\ H_2O$ calcined at different temperatures

O–H stretching vibration a part of it also occurs in the form of long range hydrogen bonded OH groups as revealed by absorption bands at 2910 cm^{-1}, 2820 cm^{-1} and 2210 cm^{-1}. The $Co(H_2O)_4Cl_2$ octahedra for pink crystals of $CoCl_2 \cdot 6H_2O$ or $CoCl_2 \cdot 4H_2O$ becomes $Co(Cl)_4(H_2O)_2$ octahedra for blue-violet $CoCl_2 \cdot 2H_2O$ where the two water molecules occupy the vertices of the octahedron and four chlorine atoms at the corners of distorted square planes which forms a chain along *b* – axis [1, 10]. Each chain is joined together by H_2O molecules *via* long distance hydrogen bonds along *a* – axis. The internal vibration of co-ordinated water molecules manifests itself in the displacement of stretching frequency to lower values [11]. Further loss of such weakly bonded H_2O molecules at 400°C leads to squeezing of the distance between two chains of $CoCl_2$ as the metal ions are joined together by one molecule of water through H bonds of shorter distance. This is evident from the appearance of broad band from 3620 to 3400 cm^{-1}. Like XRD pattern which does not reveal any complete transformation to either monohydrate or anhydrous salt at this temperature, the spectrum exhibits the presence of some long distance H-bonds (3200 cm^{-1}, 3000 cm^{-1} and

2900 cm^{-1}) typical of dihydrate salt [11]. At 500°C though a considerable extent of dechlorination takes place, the residual salt exhibits IR absorption bonds for O–H vibration suggesting that the presence of water is essential for the decomposition of $CoCl_2$. The lattice vibration of tetragonal Co_2O_3 manifests itself by a number of distinct absorption bands in the range of 800–300 cm^{-1}. As more $CoCl_2$ decomposes at 600°C both stretching and bending H–O–H vibrations not only broaden but also diminish in their intensities. A distinct oxide spectrum consisting of a mixture of Co_2O_3 and Co_3O_4 appears [12].

Diffuse reflectance spectra

The diffuse reflectance spectra of undried $CoCl_2 \cdot xH_2O$ and its products of dehydration of different temperatures were taken according to the procedure described in the previous communication [7] using boric acid and magnesium carbonate as standard or background materials. Figure 6 illustrates the typical reflectance spectra of samples with magnesium carbonate as standard substance. Although both the standard materials gave almost similar nature of spectra peak minima positions tend to shift marginally to higher energy in boric acid as given in Table 4. For undried salt the minima around 618 nm is quite strong in boric

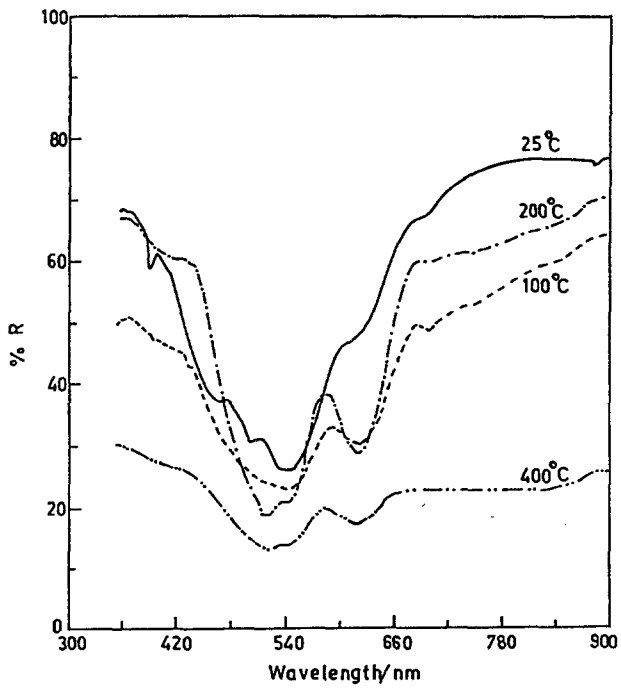

Fig. 6 Diffuse reflectance spectra of $CoCl_2 \cdot 7.33\ H_2O$ calcined of different temperatures using boric acid as standard

Table 4 Minima in diffuse reflectance spectra and the ligand field parameters for $CoCl_2 \cdot xH_2O$ and its intermediate products of dehydration

$CoCl_2 \cdot xH_2O$		100°C		200°C		400°C		Assignment
in $MgCO_3$	in boric acid	in $MgCO_3$	in boric acid	in $MgCO_3$	in boric acid	in $MgCO_3$	in boric acid	of
nm	nm	nm	nm	nm	nm	nm	nm	minima
885.3	–	–	–	–	–	–	–	–
693.7	686.5	697.5	686.5	–	689.5	–	–	$^2T_{1g}(H) \leftarrow {}^4T_{1g}$
611.0	618.0	622.5	618.0	622.5	618.0	619.0	617.0	$^4A_{2g} \leftarrow {}^4T_{1g}$
540.0	540.5	540.0	540.5	539.2	524.0	539.2	–	$^4T_{1g}(P) \leftarrow {}^4T_{1g}$
500.4	502.5	506.0	502.5	521.2	–	521.2	514.0	–
468.7	–	–	–	–	–	–	–	$^2A_{1g}(H) \leftarrow {}^4T_{1g}$
392.2	350.7	–	350.7	–	–	–	–	$^2E_g(H) \leftarrow {}^4T_{1g}$
			Ligand field parameters					
909	899	892	899	892	899	897	901	Dq / cm^{-1}
873	874	877	874	879	913	877	937	B / cm^{-1}
1.04	1.03	1.02	1.03	1.01	0.98	1.02	0.96	Dq/B
7272	7192	7139	7192	7139	7172	7176	7208	CF SE / cm^{-1}

acid the one at 611 nm in $MgCO_3$ appears as a shoulder. On the other hand, several weak but distinct minima are observed in the range of 300–540 nm with $MgCO_3$ as standard material; they are either poorly resolved or absent in boric acid. These minima are mostly due to spin-forbidden transitions to higher energy level [13]. In contrast, for 100°C heated samples a broad minima appears in the region of 500–540 nm in $MgCO_3$ due to major structural change in partially dehydrated (mainly dihydrate) product. According to Wendlandt [14] and also Grindstaff and Fogel [1] transformation from octahedral co-ordination to tetrahedral $Co[CoCl_4]$ takes place until pure octahedral $CoCl_2$ is formed. Distinct appearance of bluish patches in the samples heated at temperatures above 200°C supports this view. Since it was very difficult to obtain spectra of purely anhydrous $CoCl_2$ due to high hygroscopic nature of the salt, the spectra above 200°C is always a mixture of tetrahedral and octahedral complexes. This renders the task of assigning the peak minima for electronic transitions difficult. Despite this the most strong minima present in all the spectra around 618 nm and 540 nm have been assigned to $^4A_{2g} \leftarrow {}^4T_{1g}(F)$ and $^4T_{1g}(P) \leftarrow {}^4T_{1g}(F)$ transitions respectively from which the ligand field parameters were calculated as follows:

$$^4A_{2g} \leftarrow {}^4T_{1g}(F) = 18Dq$$

$$^4T_{1g}(P) \leftarrow {}^4T_{1g}(F) = 6Dq + 15B$$

$$CFSE = 8Dq$$

The results given in Table 4 show that there is no significant variation in ligand field parameters between the two standard materials. However, the low

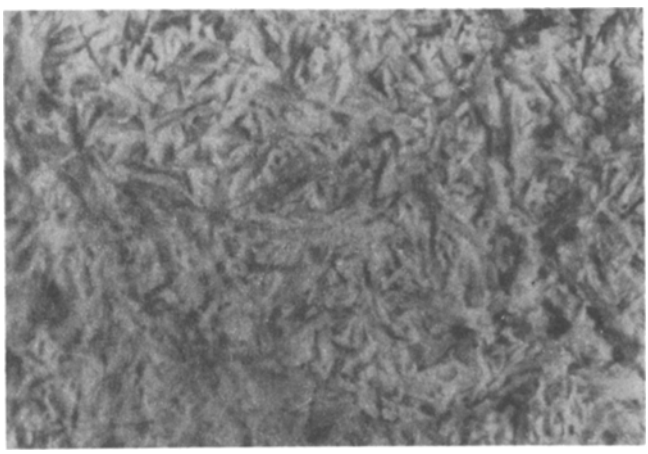

Fig. 7 Optical (stereo) and scanning electron micrographs (SEM) $CoCl_2 \cdot 7.33\ H_2O$ calcined at different temperatures. a) Stereomicrograph of sample calcined at 250°C×50

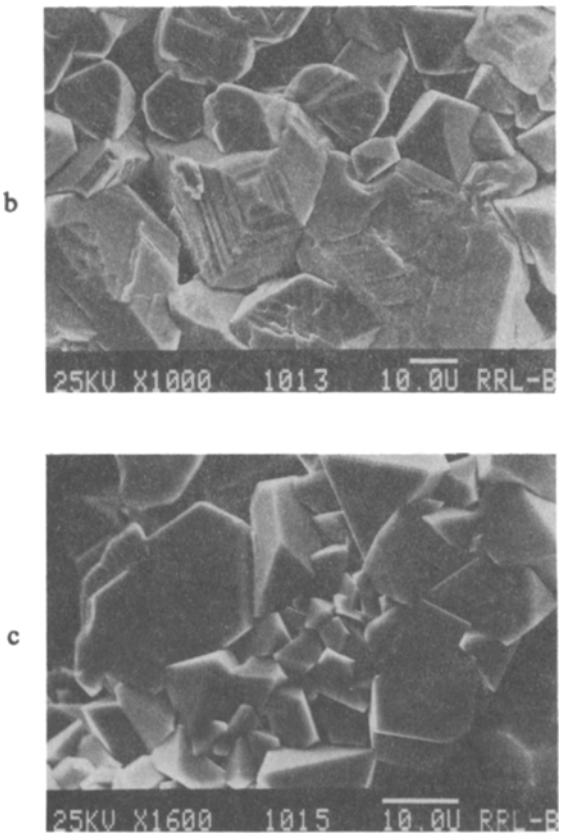

Fig. 7 Optical (stereo) and scanning electron micrographs (SEM) $CoCl_2 \cdot 7.33\ H_2O$ calcined at different temperatures. b, c) SEM of sample calcined at 850°C.

values of Dq/B ratio is a clear indication of tetragonal distortion along the major axis due to coordination of H_2O at the apices of octahedron.

Morphological characteristics

The morphology of the partially dehydrated products could not be studied by scanning electron microscopy because of the evolution of water vapour under vacuum. This resulted in the considerable haziness in the microphotographs. Therefore, an attempt was made to study the morphological behaviour of such samples under a stereomicroscope (Leitz, Germany). In general, similar morphological behaviour was observed at all temperatures in the range of 150°–400°C. A typical stereomicrograph of the sample calcined at 250°C for 1 h is shown in Fig. 7a which suggests high microporosity caused by extensive

Table 5 Thermodynamic data of the dehydration of hydrated cobalt chloride in air and flowing nitrogen environments

Dehydration of $CoCl_2 \cdot 7.33H_2O$							
Environment	DTA peak temperature T /K	Melting or number of H_2O loss	$\Delta H \pm 10$ / kJ·mol^{-1}		$\Delta S \pm 20$ / J·mol^{-1}·K^{-1}		$\Delta G_T^{\circ g)}$ at DTA peak temperature kJ·mol^{-1}
			Calculated	Found[c)]	Calculated	Found[f)]	
air	403	0.70	28.7[a)]	20.0	77.0[d)]	55.6	2.4
N_2	398	0.75	30.8[a)]	20.5	112.8[d)]	57.1	2.5
air	443	3.40	139.7[a)]	123.2	374.7[d)]	337.3	26.2
N_2	438	3.58	147.1[a)]	128.7	394.5[d)]	347.2	25.1
air	473	1.23	50.5[a)]	45.6	135.5[d)]	127.7	14.8
N_2	468	1.20	49.3[a)]	51.1	132.2[d)]	136.1	12.6
air	513	1.00	55.2[b)]	85.5	150.4[e)]	209.5	22.0
N_2	513	1.30	71.7[b)]	83.4	195.5[e)]	218.1	28.5

Table 5 Continued

Dehydration of $CoCl_2 \cdot 5.88H_2O$							
Environ-	DTA peak temperature	Melting or number of	$\Delta H \pm 10$ / $kJ \cdot mol^{-1}$		$\Delta S \pm 20$ / $J \cdot mol^{-1} \cdot K^{-1}$		$\Delta G_T^{g)}$ at DTA peak temperature
ment	T /K	H_2O loss	Calculated	Found[c)]	Calculated	Found[f)]	$kJ \cdot mol^{-1}$
air	353	melting	–	50.0	–	–	–
N_2	353	melting	–	54.0	–	–	–
air	423	3.50	143.8[a)]	124.4	385.7[d)]	340.0	19.3
N_2	423	3.35	137.7[a)]	100.0	368.8[d)]	280.0	18.3
air	453	1.18	48.5[a)]	37.8	130.0[d)]	106.4	10.4
N_2	453	1.30	53.4[a)]	40.5	143.3[d)]	114.8	11.5
air	503	1.20	66.2[b)]	64.3	180.5[e)]	176.6	24.5
N_2	503	1.23	67.9[b)]	63.7	185.0[e)]	176.6	25.1

(a) Calculated on the basis of 41.1 $kJ \cdot mol^{-1}$ as latent heat of evaporation of water.

(b) Calculated on the basis of 55.2 $kJ \cdot mol^{-1}$ as the heat of sublimation of water from ice-like structure.

(c) Obtained from area under DTA peak.

(d) Calculated on the basis of 110.2 $J \cdot mol^{-1} \cdot K^{-1}$ as entropy of evaporation of water.

(e) Calculated on the basis of 150.4 $J \cdot mol^{-1} \cdot K^{-1}$ as entropy of sublimation from ice-like structure.

(f) Calculated by using the values of ΔH and ΔG in columns 5 and 8 respectively.

(g) Calculated by using the values of ΔH and ΔS in columns 4 and 6 respectively.

dehydration and consequent shrinkage of the particles. However, SEM micrographs (JEOL, model 35 CF) of the sample calcined at 800°C reveal a host of interesting features (Figs 7b and 7c) mostly belonging to Co_3O_4 spinel and some Co_2O_3 structures. Spinel oxides such as Fe_3O_4, Mn_3O_4, Mg_2AlO_4 etc. occur in octahedral habits [15]. The prismatic structures in the figures are the broken {111} faces of the octahedrons. The thin edges (occasionally shining) around the triangles are {110} faces commonly observed in disseminated mass. A few rhombohedral crystals of Co_2O_3 can also be located. The most interesting feature of Fig. 7b is the clear evidence of the laminated growth of spinel octahedron.

Thermodynamics of dehydration

Thermodynamic functions of the dehydration of the two samples of $CoCl_2$ hydrate were estimated according to the procedure described in the previous communication [7]. Heats of different steps of dehydration were determined from the DTA peak areas after due calibration of the instrument with different substances of known heats of reaction or transformation. The results in Table 5 lend support to the proposition made in the proceeding paragraphs that evaporation of weakly coordinated molten water of crystallization is the primary mechanism of the initial stage of dehydration. However, high experimental heats of removal of the last 1.0–1.3 mol of water from undried sample do not agree well with the values calculated from either latent heat of evaporation or sublimations of water from strongly coordinated ice like structure of water of hydration. Grindstaff and Fogel [1] also found similar high enthalpy value (73.5 $kJ \cdot mol^{-1}$) for the loss of last molecule of water from $CoCl_2 \cdot 6H_2O$. Since in the present case loss of this water does not lead to the formation of anhydrous salt (rather to monohydrate in air) high ΔH value indicate possible loss of chlorine due to pyrohydrolysis of $CoCl_2$ by loosely bound H_2O in undried sample. On the other hand, for $CoCl_2 \cdot 5.88\ H_2O$, loss of last 1.2–1.3 mol of water leads to the formation of anhydrous salt. In such case the experimental value of the heat of dehydration agrees well with the heat of sublimation of water from ice-like structure.

The above observation on the differences in the behaviour of thermal dehydration of $CoCl_2$ hydrates containing more or less than six molecules of water of crystallization raises some question on the molecular and crystal structure of di- and mono-hydrate salt. Infrared spectra and heats of dehydration of di- and monohydrates indicate the presence of H bonded OH groups. It is proposed that the linear bonding of the water molecules possibly act as bridges between two Co(II) in the two adjacent octahedral polymeric chains containing chloride ions at the four corners of square plane as follows:

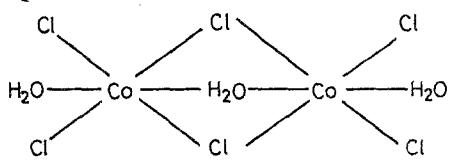

In monohydrate salt hydrogen bonding between the lone water molecule in $Co(Cl)_5H_2O$ octahedra possibly occurs in the following manner:

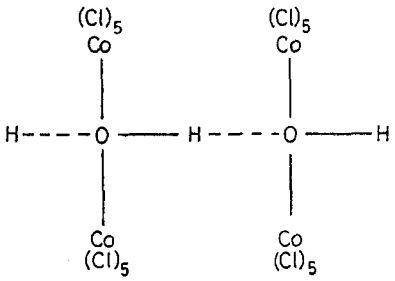

Entropy changes for different steps of dehydration (Table 5) for partially dried sample show excellent agreement between calculated and found values.

* * *

The authors wish to express their sincere thanks to Mr. D. N. Ney, head of Pyrometallurgy Division for his keen interest and support during the course of investigation. Thanks are also due to Director R. R. L. Bhubaneswar for his kind permission to publish the paper. One of the authors is thankful the CISR, New Delhi for awarding a Junior Research Fellowship.

References

1 W. K. Grindstaff and N. Fogel, J. Chem. Soc. (Dalton Trans), (1972) 1476.
2 N. S. Akhmetov, General and Inorganic Chemistry (Eng. Transl.), Mir Publishers, Moscow 1983, p. 597.
3 H. J. Borchardt and F. Daniels, J. Phys. Chem., 61 (1957) 917.
4 E. L. Simmons and W. W. Wendlandt, Thermochim. Acta, 3 (1971) 25.
5 J. R. Williams and W. W. Wendlandt, Thermochim. Acta, 7 (1973) 275.
6 J. Ribas, A. Escuer, M. Serra and R. Vicente, Thermochim. Acta, 102 (1986) 125.
7 S. K. Mishra and S. B. Kanungo, J. Thermal Anal., 38 (1992) 2417.
8 A. Volsky and E. Sergievskaya, Theory of Metallurgical Processes; Pyrometallurgical Processes (Eng. Transl.), Mir Publishers, Moscow 1971, p. 273.
9 O. Kubaschewsky and L. L. Evans, Metallurgical Thermochemistry, Pergamon Press, New York 1959.
10 R. W. G. Wyckoff, Crystal structure, Vol. 3, 2nd Ed., Interscience, New York 1965, pp. 788–789.
11 Ya. I. Ryskin, Infrared spectra of Minerals (V. C. Farmer Ed.), Mineralogical Soc., London 1974, pp. 164–167.
12 F. F. Bently, L. D. Smithson and A. L. Rozcek, Infrared Spectra and Characteristic Frequencies (700–300 cm^{-1}) Interscience, New York 1968, Sptm. No. 1516.
13 N. S. Hush and R. J. M. Hobbs, "Progress in Inorganic Chemistry" F. A. Cotton (Ed.) Vol.10, Interscience, New York 1968,pp. 259–313.
14 W. W. Wendlandt, Thermal Analysis, 3rd Ed., John Wiley & Sons, New York 1986, p. 575.
15 A. Milovsky and O. V. Konorov, Mineralogy (Engl. Transl.), Mir Publishers, Moscow 1985, p. 144.

Zusammenfassung — Mittels isothermer und nichtisothermer Massenverlustmethoden wurden die Dehydratation und die Zersetzung von ungetrockneten und teilweise getrockneten Proben von hydratiertem $CoCl_2$ untersucht. Mittels Elementaranalyse, Röntgendiffraktion, Mikroskopie, IR- und Remissionsspektroskopie wurden die Zwischenprodukte von Dehydratation und Zersetzung bei verschiedenen Temperaturen charakterisiert. Obwohl die Röntgendiffraktion bei der eindeutigen Identifizierung der Bildung des Basissalzes versagte, zeigten die IR-Spektren die Existenz von wasserstoffgebundenen OH-Gruppen in Proben, die auf 500°-600°C erhitzt wurden. Dies wird weiterhin durch die Remissionsspektren der "dehydratierten" Proben bestätigt, welche tetragonal deformierte Koordinierungsstrukturen zeigt, die der Gegenwart von H_2O zuzuschreiben sind. Im Hinblick auf strukturelle Veränderungen in den dehydratierten Salzen wurden thermodynamische Funktionen für verschiedene Schritte der Dehydratation berechnet und diskutiert.